$S=\frac{1}{2}$ alternating chain using multiprecision methods

T. Barnes
Physics Division, Oak Ridge National Laboratory, Oak Ridge, Tennessee 37831-6373
and Department of Physics and Astronomy, University of Tennessee, Knoxville, Tennessee 37996-1501

J. Riera
Instituto de Fisica Rosario, 2000 Rosario, Argentina

D. A. Tennant
Solid State Division, Oak Ridge National Laboratory, Oak Ridge, Tennessee 37831-6393

(Received 3 February 1998; revised manuscript received 7 October 1998)

In this paper we present results for the ground state and low-lying excitations of the $S=1/2$ alternating Heisenberg antiferromagnetic chain. Our more conventional techniques include perturbation theory about the dimer limit and numerical diagonalization of systems of up to 28 spins. An application of multiple precision numerical diagonalization allows us to determine analytical perturbation series to high order; the results found using this approach include ninth-order perturbation series for the ground state energy and one magnon gap. We also determine the fifth-order dispersion relation and third-order exclusive neutron scattering structure factor for one-magnon modes and numerical and analytical binding energies of $S=0$ and $S=1$ two-magnon bound states. [S0163-1829(99)02917-3]

I. INTRODUCTION

The alternating Heisenberg chain (AHC) is a simple quantum spin system that can be used to model the magnetic behavior of a wide range of materials; Table I gives some representative examples of alternating chains. This model is a straightforward generalization of the uniform Heisenberg antiferromagnetic chain, which is the most widely studied quantum spin system. The uniform $S=1/2$ chain has a gapless excitation spectrum with a known dispersion relation and a rather complicated ground state which is characterized by strong quantum fluctuations, making it highly unstable to perturbations.

The alternating chain generalizes the uniform chain by alternating the spin-spin interaction between two values J_1 and J_2. Since the alternating chain Hamiltonian is rotationally invariant with respect to spin, the total spin is a good quantum number, and the (antiferromagnetic) ground state is a spin singlet. The translational symmetry of the uniform one-dimensional (1D) chain, however, is reduced by dimerization, and the resulting system has a gap to the first excited state, which has $S=1$. This lowest excitation is part of a ''one-magnon'' triplet band. The alternating chain has a rather complicated spectrum of states at higher energies, including multimagnon continua and bound states.

The alternating chain is of theoretical interest as a simple 1D isotropic quantum spin system with a gap, which presumably is qualitatively similar to other more complicated systems such as integer-spin chains and even-leg $S=1/2$ spin ladders. The approach to the uniform chain limit is also of interest as an example of critical behavior. Finally, the alternating chain is useful as a model for the application of new numerical techniques such as the multiprecision approach introduced here.

The alternating chain Hamiltonian is realized in nature in many materials that have two important but structurally inequivalent superexchange paths that are spatially linked, so that a series of spin-spin interactions of strength $J_1-J_2-J_1-J_2\cdots$ results. Examples of materials of this type are $(VO)_2P_2O_7$ and $Cu(NO_3)_2\cdot 2.5H_2O$ and various aromatic free-radical compounds.[1]

Alternating chains may also arise as a result of the spin-Peierls effect. In the 1D Heisenberg antiferromagnet a spatial dimerization of the ion positions along the chain gives alternating interaction strengths, which results in a lowering of the magnetic ground state energy. There is a corresponding increase in the lattice energy (the phonon contribution) which dominates at large distortions. In the combined magnetic-phonon system an equilibrium is reached at a spatial dimerization that minimizes the ground state energy. This spontaneous dimerization is known as the spin-Peierls effect, and the resulting magnetic Hamiltonian is an alternating Heisenberg chain. Examples of spin-Peierls alternating chains in nature are $CuGeO_3$ and α'-NaV_2O_5.

Much of the recent interest in alternating chains arises

TABLE I. Representative alternating chain materials. The parameters $\mathcal{J}=(1+\alpha)J/2$ and $\delta=(1-\alpha)/(1+\alpha)$ are also commonly used (see text).

Material	J (meV)	α	Reference
$Sr_{14}Cu_{24}O_{41}$	11.2	$-0.10(1)$	28,33
$Cu(NO_3)_2\cdot 2.5H_2O$	0.45	0.27	20,29
$(VO)_2P_2O_7$	≈ 10	0.8	4
$CuWO_4$	≈ 12	≈ 0.9	31
α'-NaV_2O_5	40	0.9	32
$CuGeO_3$ [a]	13	0.94	30

[a]There may also be important second nearest neighbor interactions in this material.

from the observation of a spin-Peierls effect in $CuGeO_3$.[2] Many experimental studies suggest an alternating chain interaction in $CuGeO_3$ (see for example Ref. 3 and references cited therein), although interactions beyond nearest neighbor are also thought to be important. The observation of a two-magnon continuum in $CuGeO_3$ with an onset close to 2Δ,[3] where Δ is the magnon energy-gap at the zone center, has motivated recent theoretical studies of the continuum and two-magnon bound states in the AHC. Added impetus has come from neutron scattering studies of $(VO)_2P_2O_7$,[4,5] which show that this material is dominantly an alternating chain and provide evidence of a possible $S=1$ two-magnon bound state.

In this paper we present a detailed study of the AHC, including results for the ground state and low-lying excitations. We begin by introducing the model (Sec. II) and reviewing previous studies (Sec. III). Perturbation theory about the dimer limit, which we find to be particularly well suited to studying the AHC, is introduced in Sec. IV A and applied to the ground state energy E_0, excitation gap $E_{\rm gap}$, and one-magnon dispersion $\omega(k)$ in Sec. IV B. Section IV C summarizes analytical predictions for the critical behavior of the gap and ground state energy. Section V presents our numerical results for energies; Sec. V A gives Lanczos results, and Sec. V B introduces a new numerical method for abstracting analytical perturbation series from high precision numerical results. In Sec. V B we use this approach to give series (based on $L=20$ diagonalization) to $O(\alpha^9)$ for E_0, $E_{\rm gap}$, and the zone-boundary energy $E_{\rm ZB}$. Previously these series had only been published to $O(\alpha^3)$. We also used this multiple precision method to determine the series expansion of $\omega(k)$ to $O(\alpha^5)$. These high-order formulas are accurate over a wide range of alternations and should prove useful to experimentalists. The critical behavior is studied in Sec. V C, and we present relationships between the derivatives of E_0 and $E_{\rm gap}$ at the critical point as well as comparing our results to the proposed scaling behavior of these quantities. Two-magnon bound states exist in the AHC, which is a convenient model for the study of this type of excitation. We discuss the binding mechanism and give second-order formulas for binding energies in Sec. VI. Since neutron scattering can give detailed information on the excitations of alternating chains, we derive general expressions for the exclusive neutron scattering structure factor $\mathcal{S}(k)$ to a specific excitation (Sec. VII A). We apply these results to the excitation of the one-magnon band in Sec. VII B, and use the multiprecision method to calculate this $\mathcal{S}(k)$ to $O(\alpha^3)$. A short discussion of the rather complicated neutron excitation of the two-magnon bound state band is given in Sec. VII C. In Sec. VIII we present an illustrative application of our new formulas to a real material, the alternating chain compound $(VO)_2P_2O_7$, for which single-crystal neutron scattering data is available. Finally we summmarize our results and present our conclusions in Sec. IX.

II. THE MODEL

The AHC Hamiltonian is

$$H=\sum_{i=1}^{L/2} J_1\vec{S}_{2i-1}\cdot\vec{S}_{2i}+J_2\vec{S}_{2i}\cdot\vec{S}_{2i+1}. \tag{1}$$

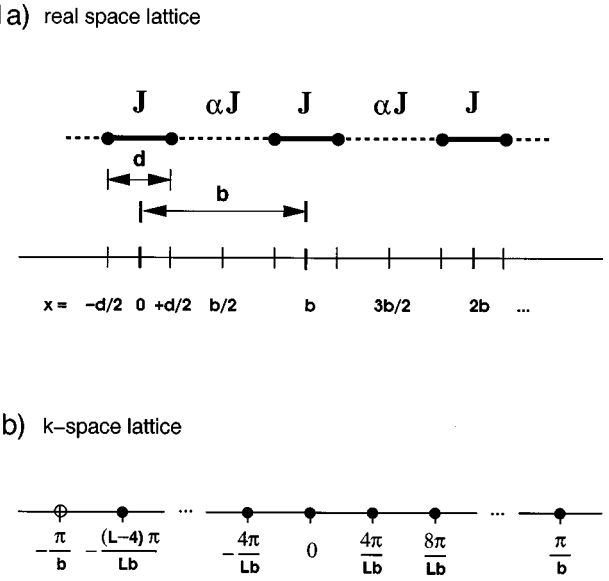

FIG. 1. The geometry of a 1D alternating chain. The internal dimer spin-spin interaction (solid line) is $J_1=J$ and the dimer extent is d. The spin-spin coupling between dimers (dashed line) is $J_2=\alpha J$, and the spacing between dimer centers, which is the length of the unit cell, is b. A spatially uniform chain has a smaller unit cell length of $d=b/2$, which is normally called a.

In this paper we impose periodic boundary conditions, with spins 1 and $L+1$ identified. We usually assume that $J_1>J_2>0$, so we are in a regime of coupled antiferromagnetic dimers.

We can also write this in terms of $J_1\equiv J$ and the alternation α, where $J_2\equiv\alpha J$,

$$H=\sum_{i=1}^{N_d=L/2} J\vec{S}_{2i-1}\cdot\vec{S}_{2i}+\alpha J\vec{S}_{2i}\cdot\vec{S}_{2i+1}. \tag{2}$$

N_d is the number of independent dimers or unit cells, which are coupled by the interaction αJ. An equivalent form often used in the discussion of spin-Peierls transitions writes this as interactions of strength $\mathcal{J}(1+\delta)$ and $\mathcal{J}(1-\delta)$, which are related to our definitions by $\mathcal{J}=(1+\alpha)J/2$ and $\delta=(1-\alpha)/(1+\alpha)$.

For $\alpha=1$ this system is an isotropic, uniform, $S=1/2$ Heisenberg chain which has gapless excitations, and for $\alpha=0$ it reduces to uncoupled dimers with $E_{\rm gap}=J$. Since this is an isotropic Hamiltonian with antiferromagnetic couplings, for $\alpha>0$ we expect an $S=0$ (singlet) ground state and an $S=1$ (triplet) band of magnons as the first excitation.

The geometry of our alternating chain is shown in Fig. 1. Note that the unit cell has length b; this leads to a different set of momenta than the more familiar uniform chain, which has a unit cell of $a=b/2$. Since the Hamiltonian is invariant under translations by multiples of b, the allowed momenta are

$$k_n=\frac{n}{L/4}\frac{\pi}{b}. \tag{3}$$

For $L/2$ even the index n takes the values $n=0,\pm1,\pm2,\ldots,\pm(L/4-1),L/4$; for $L/2$ odd the series stops with $\pm{\rm int}(L/4-1)$. There are $L/2=N_d$ independent momenta be-

cause there are N_d invariant translations of H. Positive and negative k levels are degenerate as usual due to reflection symmetry.

III. PREVIOUS STUDIES

Early numerical studies of the zero temperature alternating chain by Duffy and Barr[6] and Bonner and Blöte[7] considered the ground state energy and triplet gap on chains of up to 10 and 12 spins, respectively. They concluded that this system probably had a gap for any nonzero alternation. Duffy and Barr also gave results for the ground-state nearest-neighbor correlation function, magnetization in an external field, and triplet dispersion relation $\omega(k)$. Coupled cluster expansions of the ground-state energy and zero-temperature magnetization and susceptibility have since been carried out to high order in α by Kohmoto *et al.*[8] in a series of studies of an anisotropic generalization of the alternating chain. Gelfand, Singh, and Huse[9] also used coupled cluster methods to generate a high-order series for the ground state energy. A principal concern of Bonner and Blöte and subsequent numerical work was to test the critical behavior of the uniform chain limit; analytical studies had predicted that the gap $E_{\rm gap}/\mathcal{J}$ should open as $\delta^{2/3}$ times logarithmic corrections for small alternation,[10] and that the bulk-limit ground-state energy per spin expressed in terms of $\mathcal{J}$ and δ, $\tilde{e}_0 = E_0/\mathcal{J}L = 2e_0/(1+\alpha)$, should approach $1/4-\ln(2)$ as $\delta^{4/3}$ times logarithmic corrections.[11,12] The dependence of $\tilde{e}_0$ on δ is important in determining the existence of a spin-Peierls transition in an antiferromagnetic chain coupled to the phonon field.[7]

Numerical studies on larger systems were subsequently carried out by Soos *et al.*[13] (to $L=26$ for e_0 and $L=21$ for $E_{\rm gap}$) and Spronken *et al.*[14] (to $L=18$). Spronken *et al.* supported the anticipated critical behavior. Soos *et al.*, however, considered much smaller δ and larger lattices and concluded that the expected asymptotic form was incorrect. This issue is unresolved and merits future study on much larger systems.

More recent studies of the alternating chain model were motivated by experimental work on $CuGeO_3$.[2,3] In particular the question of possible two-magnon bound states has been of interest; an analytical paper by Uhrig and Schulz[15] anticipates an $S=0$ bound state for all δ and an $S=1$ bound state ''around $k=\pi/2$'' (our $k=\pi/b$, the zone boundary) ''for not too small δ.'' Bouzerar *et al.*[17] similarly conclude that the $S=1$ two-magnon bound state only exists for a range of k around the zone boundary. Fledderjohann and Gros[18] have searched for evidence of such bound states in a numerical study of the structure factor $S(k,\omega)$ on chains of up to $L=24$, and conclude that an $S=1$ two-magnon bound state does indeed lie below the two-magnon continuum for all δ.

Numerical studies of the thermodynamic properties of the alternating chain have received much less attention. Duffy and Barr gave results for the internal energy, entropy, specific heat, and magnetic susceptibility of an $L=10$ chain for a range of alternations. Diederix *et al.*[20] specialized to the parameter $\alpha=0.27$ appropriate for $Cu(NO_3)_2\cdot 2.5H_2O$ and gave results for the magnetization, susceptibility, and entropy on systems of up to $L=12$. Barnes and Riera[21] gave results for the susceptibility on chains of up to $L=16$, and extrapolated to the bulk limit for values of $\alpha\approx 0.6$–0.8 considered appropriate for $(VO)_2P_2O_7$.

IV. ANALYTICAL RESULTS

A. Dimer perturbation theory

Analytical results for the alternating chain can be derived using perturbation theory about the isolated dimer limit. For this purpose we partition the Hamiltonian into a dimer H_0 and an interdimer interaction H_I,

$$H_0 = \sum_{i=1}^{N_d} J\vec{S}_{2i-1}\cdot\vec{S}_{2i}, \tag{4}$$

$$H_I = \sum_{i=1}^{N_d} \alpha J\vec{S}_{2i}\cdot\vec{S}_{2i+1}. \tag{5}$$

The single-dimer eigenstates of H_0 are an $S=0$ ground state $|\bigcirc\rangle = (|\uparrow\downarrow\rangle - |\downarrow\uparrow\rangle)/\sqrt{2}$ with $E_0^{(\rm dimer)} = -3J/4$ and an $S=1$ triplet of dimer excitations ''excitons'' $\{|(+)\rangle, |(0)\rangle, |(-)\rangle\}$, with $E_1^{(\rm dimer)} = +J/4$. We label these excitations by the dimer S_z, for example $|(0)\rangle = (|\uparrow\downarrow\rangle + |\downarrow\uparrow\rangle)/\sqrt{2}$. The ground state of the full H_0 is a direct product of $S=0$ dimer ground states

$$|\psi_0^{(0)}\rangle = \prod_{m=1}^{N_d} |\circ_m\rangle \equiv |0\rangle, \tag{6}$$

with an energy of $E_0 = N_d\cdot E_0^{(\rm dimer)} = -3JL/8$.

Similarly, the unperturbed one-magnon state with momentum k and $S_z=+1$ is given by

$$|\psi_1^{(0)}(k)\rangle^{(+)} = \frac{1}{\sqrt{N_d}}\sum_{m=1}^{N_d} e^{ikx_m}|(+)_m\rangle. \tag{7}$$

(We will suppress the redundant polarization superscript on $|\psi_1\rangle$ subsequently.) We take the location x_m of dimer m to be the midpoint of the two spins. In this and similar state vectors, if the state of any dimer n is not specified explicitly it is in the ground state $|\circ_n\rangle$.

It is useful to derive the effect of H_I on dimer product basis states. For example, operating with H_I on the H_0 ground state Eq. (6) gives

$$H_I\,|0\rangle = \frac{J\alpha}{4}\sqrt{3}\sum_{m=1}^{N_d}\underbrace{|(0,0)_{m,m+1}\rangle}_{\text{double excite}}, \tag{8}$$

where

$$|(0,0)_{m,m+1}\rangle = \frac{1}{\sqrt{3}}(|(+)_m(-)_{m+1}\rangle - |(0)_m(0)_{m+1}\rangle + |(-)_m(+)_{m+1}\rangle) \tag{9}$$

is a state of two neighboring $S=1$ dimer excitons at dimer sites $m,m+1$ coupled to give $(S,S_z)=(0,0)$. Similarly the

effect of H_I on a single $S_z=+1$ exciton at dimer site m gives

$$H_I\,|(+)_m\rangle = \frac{\alpha J}{4}\Big\{ \underbrace{-|(+)_{m-1}\rangle - |(+)_{m+1}\rangle}_{\text{hop}}$$

$$\underbrace{-|(+)_{m-1}(0)_m\rangle + |(0)_{m-1}(+)_m\rangle}_{\text{excite}}$$

$$\underbrace{-|(+)_m(0)_{m+1}\rangle + |(0)_m(+)_{m+1}\rangle}_{\text{excite}}$$

$$+\sqrt{3}\sum_{m'=1}^{N_d}{}' \underbrace{|(+)_m(0,0)_{m',m'+1}\rangle}_{\text{double excite}}\Big\}\,. \tag{10}$$

The prime on the sum indicates that all dimer sites represented in the state are distinct, so in this case $m'\neq m,m-1$. Evidently H_I both translates the exciton (leading to momentum eigenstates) and couples it to two-exciton and three-exciton states of higher unperturbed energy. The specific polarization state $(|(+)(0)\rangle-|(0)(+)\rangle)/\sqrt{2}$ is forced because this is the unique $|S=1,S_z=1\rangle$ combination of two $S=1$ dimers. We abbreviate this state as $|(1,1)_{m,n}\rangle$, specifying the S_{total} and $S_{z\ \text{total}}$ and the excited dimers m and n $(m<n)$, which gives the simplified form

$$H_I|(+)_m\rangle = -\frac{\alpha J}{4}\Big\{ |(+)_{m-1}\rangle + |(+)_{m+1}\rangle + \sqrt{2}(|(1,1)_{m-1,m}\rangle + |(1,1)_{m,m+1}\rangle) - \sqrt{3}\sum_{m'=1}^{N_d}{}' |(+)_m(0,0)_{m',m'+1}\rangle\Big\}. \tag{11}$$

We can use this formalism to generate an expansion in α for the ground state and excitations and their matrix elements using standard quantum mechanical perturbation theory. These results are presented in the next section.

B. Perturbative results for E_0, E_{gap}, and $\omega(k)$

The perturbative generalization of the ground state Eq. (6) to $O(\alpha^2)$ is

$$|\psi_0\rangle = \eta_0\Big[|0\rangle + \alpha\Big\{-\frac{\sqrt{3}}{8}\sum_{m=1}^{N_d}|(0,0)_{m,m+1}\rangle\Big\} + \alpha^2\Big\{-\frac{\sqrt{3}}{32}\sum_{m=1}^{N_d}|(0,0)_{m,m+1}\rangle - \frac{\sqrt{3}}{32}\sum_{m=1}^{N_d}|(0,0)_{m,m+2}\rangle + \frac{1}{16}\sqrt{\frac{2}{3}}\sum_{m=1}^{N_d}|(0,0)_{m,m+1,m+2}\rangle + \frac{3}{128}\sum_{m,m'=1}^{N_d}{}'|(0,0)_{m,m+1}(0,0)_{m',m'+1}\rangle, \tag{12}$$

where $\eta_0=1-(3/128)\alpha^2N_d$ is the $O(\alpha^2)$ normalization. Note that three- and four-exciton states appear at $O(\alpha^2)$. The four-exciton states encountered here are two $S=0$, $(0,0)_{m,m+1}$ two-exciton pairs, again with the restriction on the sum Σ' that no excitons overlap. The three-exciton state with $(S,S_z)=(0,0)$,

$$|(0,0)_{m_1,m_2,m_3}\rangle = \frac{1}{\sqrt{6}}(|(+)_{m_1}(0)_{m_2}(-)_{m_3}\rangle + |(0)_{m_1}(-)_{m_2}(+)_{m_3}\rangle + |(-)_{m_1}(+)_{m_2}(0)_{m_3}\rangle - |(+)_{m_1}(-)_{m_2}(0)_{m_3}\rangle - |(-)_{m_1}(0)_{m_2}(+)_{m_3}\rangle - |(0)_{m_1}(+)_{m_2}(-)_{m_3}\rangle), \tag{13}$$

is the unique $S=0$ combination of three spin-one objects at adjacent sites.

Since the $O(\alpha^p)$ state determines the $O(\alpha^{2p+1})$ energy, we can in principle use Eq. (12) to derive the ground state energy to $O(\alpha^5)$. This proves to be a rather intricate calculation. We have carried out this derivation of $e_0\equiv E_0/LJ$ analytically to $O(\alpha^4)$, with the result

$$e_0(\alpha) = -\frac{3}{2^3} - \frac{3}{2^6}\alpha^2 - \frac{3}{2^8}\alpha^3 - \frac{13}{2^{12}}\alpha^4. \tag{14}$$

This series was previously evaluated analytically to $O(\alpha^3)$ by Brooks Harris,[22] and the series coefficients were determined numerically to $O(\alpha^{15})$ to 5–6 significant figures by Gelfand, Singh, and Huse[9] using a coupled cluster expansion.

A similar $O(\alpha)$ generalization of the unperturbed $S=1$ one-magnon excitation Eq. (7) gives

$$|\psi_1(k)\rangle = \eta_1\frac{1}{\sqrt{N_d}}\Big[\sum_{m=1}^{N_d}e^{ikx_m}|(+)_m\rangle + \alpha\Big\{-\frac{1}{2\sqrt{2}}\sum_{m=1}^{N_d}(e^{ikb}+1)e^{ikx_m}|(1,1)_{m,m+1}\rangle - \frac{\sqrt{3}}{8}\sum_{m,m=1}^{N_d}{}'e^{ikx_m}|(+)_m(0,0)_{m'}\rangle\Big\}\Big]. \tag{15}$$

The normalization $\eta_1=1$ to this order in α. Taking the expected value of H with this state gives a one-magnon dispersion relation of

$$\frac{\omega(k)}{J} = \Big(1-\frac{1}{16}\alpha^2+\frac{3}{64}\alpha^3\Big) - \Big(\frac{1}{2}\alpha+\frac{1}{4}\alpha^2-\frac{1}{32}\alpha^3\Big)\cos(kb) - \Big(\frac{1}{16}\alpha^2+\frac{1}{32}\alpha^3\Big)\cos(2kb) - \frac{1}{64}\alpha^3\cos(3kb). \tag{16}$$

The $O(\alpha^3)$ gap is therefore

$$\frac{E_{gap}}{J} = 1-\frac{1}{2}\alpha-\frac{3}{8}\alpha^2+\frac{1}{32}\alpha^3. \tag{17}$$

These one-magnon energies were found previously to this order by Brooks Harris,[22] and serve as a check of our $O(\alpha)$ one-magnon state Eq. (15).

C. Critical behavior

As we approach the uniform chain the ground state energy and the gap are both expected to approach their limiting values as powers of δ times logarithmic corrections.[11,12] The behavior near the critical point is usually discussed in terms of the variable

$$\delta=(1-\alpha)/(1+\alpha) \tag{18}$$

with

$$\mathcal{J}=(1+\alpha)J/2 \tag{19}$$

fixed, so the alternating couplings are $\mathcal{J}(1+\delta)$ and $\mathcal{J}(1-\delta)$. These variables are more appropriate for a spin-Peierls system because a displacement of an intermediate ion by $O(\delta)$ should increase and decrease alternate couplings by approximately the same amount. The ground state energy per spin relative to fixed $\mathcal{J}$ is $\tilde{e}_0(\delta)=2e_0/(1+\alpha)$.

The critical behavior of the ground state energy and singlet-triplet gap has been discussed by Cross and Fisher[11] and by Black and Emery.[12] The approach used was to consider the properies of the Heisenberg chain within a Luttinger-Tomonaga approximation, which involves a Jordan-Wigner transformation to a fermion representation of the spin operators, and then replacing the cosinusoidal fermion dispersion by a linear dispersion at the Fermi wave vector. This linear approximation is required to simplify the commutation relations between the density operators, allowing the interacting fermion problem to be solved. Renormalization techniques are then used to calculate the asymptotic behavior of various physical quantities within this approximation. The approach makes approximations in neglecting states far from the Fermi surface and ignoring energy renormalization effects. The predicted asymptotic δ dependence is

$$\lim_{\delta\to 0}\tilde{e}_0(\delta)-\tilde{e}_0(\delta=0)\propto\frac{\delta^{4/3}}{|\ln\delta|} \tag{20}$$

and

$$\lim_{\delta\to 0}\frac{E_{\rm gap}}{\mathcal{J}}\propto\frac{\delta^{2/3}}{|\ln\delta|^{1/2}}. \tag{21}$$

We will compare these predictions with our numerical results in the next section; it is of interest to see whether these formulas are accurate for values of δ realized by known materials.

One may derive some relations between energies and their derivatives near the critical point from a simple identity satisfied by the alternating chain Hamiltonian Eq. (2). Note the proportionality relation

$$H(J,\alpha J)=\alpha\cdot H(\alpha^{-1}J,J), \tag{22}$$

which implies for any energy eigenvalue

$$\frac{E_n(\alpha)}{J}=\alpha\frac{E_n(\alpha^{-1})}{J}. \tag{23}$$

Assuming that there are no singularities on the real axis except at $\alpha=1$, we may differentiate this relation with respect to α elsewhere. As it is expected that the singularity in $e_0(\alpha)=E_0/JL$ at the critical point $\alpha=1$ is higher order than linear, $de_0(\alpha)/d\alpha$ should be well defined everywhere; differentiating Eq. (23) with $n=0$ therefore leads to

$$\left.\frac{de_0(\alpha)}{d\alpha}\right|_{\alpha=1}=\frac{1}{2}e_0(\alpha=1)=\frac{1}{8}-\frac{\ln(2)}{2}=-0.22157\cdots. \tag{24}$$

This is consistent with the expectation that the scaled $\tilde{e}_0(\delta)$ has zero slope in δ as we approach the critical point. To see this, note that $\tilde{e}_0(\delta)=2e_0(\alpha)/(1+\alpha)$, so

$$\frac{d\tilde{e}_0(\delta)}{d\delta}=e_0(\alpha)-\frac{2}{(1+\delta)}\frac{de_0(\alpha)}{d\alpha}, \tag{25}$$

and as we approach the critical point

$$\lim_{\delta\to 0}\frac{d\tilde{e}_0(\delta)}{d\delta}=\lim_{\alpha\to 1}e_0(\alpha)-2\frac{de_0(\alpha)}{d\alpha}=0. \tag{26}$$

Successive derivatives of Eq. (23) can be used to infer relations between higher derivatives of $e_0(\alpha)$ (or other energy eigenvalues) as one approaches $\alpha=1$.

V. NUMERICAL METHODS

A. Lanczos results

Direct numerical diagonalization of moderately large systems is possible for the $S=1/2$ alternating chain. Here we used a Lanczos method[23] to obtain ground state and one-magnon energies on $L=4n$ lattices up to $L=28$. Motivated by previous numerical studies, we extrapolate these energies to bulk limits using a simple exponential-and-power estimate for the finite size dependence

$$f(\alpha,L)=f(\alpha)+c_1\frac{\exp(-L/c_2)}{L^p}, \tag{27}$$

where $p=1$ for energy gaps ($f=E_n-E_0$) and $p=2$ for the ground state energy per spin ($f=E_0/L$). We determined the finite-lattice energies to about 14 place accuracy, and fitted the $L=4(n-2),4(n-1)$ and $4n$ results to these asymptotic forms.

The resulting bulk-limit ground state energy is shown in Fig. 2 and presented in Table II, to nine figure accuracy for the smaller α values. For larger α we include the change in $e_0(\alpha)$ between $L=16,20,24$ and $L=20,24,28$ extrapolations in parenthesis after the tabulated $L=20,24,28$ result, as an error estimate. These numerical energies provide an accurate check of the perturbative formulas Eq. (14) and Eq. (28).

We also used Lanczos diagonalization on lattices up to $L=28$ to determine the singlet-triplet gap and zone boundary energy. These results are given in Table II and shown in Fig. 3, again with a systematic error estimate that is the discrepancy between $L\leqslant 24$ and $L\leqslant 28$ extrapolations. (The + sign indicates that the bulk-limit gap estimate increased with increasing L.) Our Lanczos results are again consistent with the perturbative expansions Eq. (16) and Eq. (17). The higher-order multiple precision series Eq. (29) and Eq. (30) are as expected found to be in agreement to much higher accuracy.

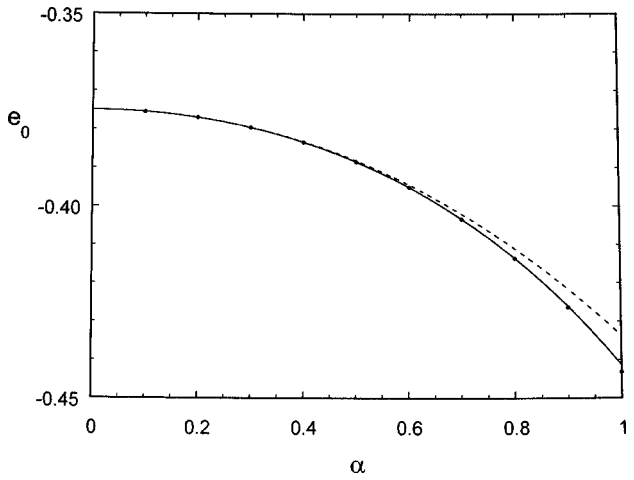

FIG. 2. Ground state energy per spin $e_0(\alpha)=E_0/LJ$ of the alternating chain. The dashed line is third-order perturbation theory, the solid line is ninth order, and the points are bulk limit extrapolations of Lanczos data.

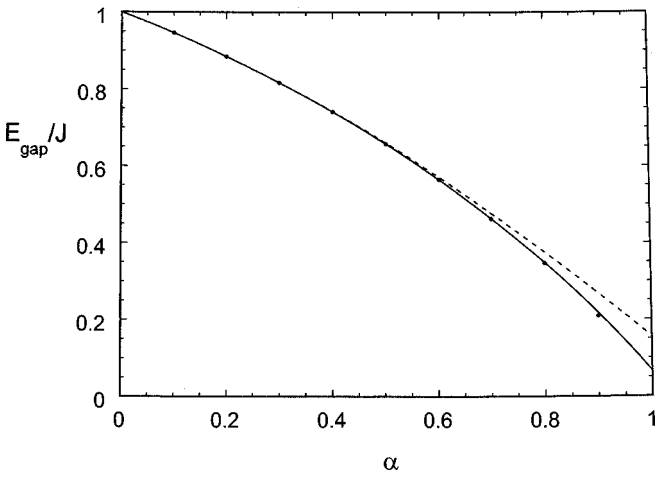

FIG. 3. Singlet-triplet energy gap $E_{\rm gap}/J$ of the alternating chain, as in Fig. 2.

B. High-order series from multiple precision

One may use numerical diagonalization combined with multiple precision programming to determine analytical perturbation series to high order. For this application of numerical methods to spin systems we employed the multiprecision package MPFUN developed by Bailey,[24] applied to our Fortran code for low-lying eigenvectors of the alternating chain using the ''modified Lanczos'' method.[25] We typically generated energies to 300 significant figures with $\alpha=10^{-30}$ (and to 400 figures for $L=20$), which allowed the perturbation expansion coefficients to be read directly from the numerical energies as rational fractions. This was possible in part because the energy denominators involved simple powers of small integers that could be anticipated. The limiting order in this approach is determined by the size of the system one can diagonalize, since the periodic boundary conditions introduce $O(\alpha^{L/2})$ finite-lattice corrections to energies. This gave a limit of $O(\alpha^9)$ for the order of the bulk limit expansion that could be determined from the largest system we diagonalized with multiple precision, $L=20$.

The multiprecision package was implemented on a Pentium PC, a DEC Alpha, and a Sun 450. Execution times for E_0 at this level of precision were approximately 6 CPU hours for $L=16$ on the DEC Alpha and 100 CPU hours for $L=20$ on the Sun 450.

The $O(\alpha^9)$ series for the ground state energy per spin determined in this manner is

$$e_0(\alpha)=-\frac{3}{2^3}-\frac{3}{2^6}\alpha^2-\frac{3}{2^8}\alpha^3-\frac{13}{2^{12}}\alpha^4-\frac{89}{2^{14}\times 3}\alpha^5 - \frac{463}{2^{17}\times 3}\alpha^6-\frac{7\times 61\times 191}{2^{22}\times 3^3}\alpha^7-\frac{11\times 139\times 271}{2^{21}\times 3^4\times 5}\alpha^8 - \frac{107\times 22\,005\,559}{2^{30}\times 3^5\times 5^2}\alpha^9 \tag{28}$$

and the $O(\alpha^9)$ series for the gap to the $k=0$ one-magnon state is

TABLE II. Bulk limit alternating chain energies ($J=1$) and two-magnon bound state binding energies, Eq. (44), extrapolated from $L=20,24,28$. The change observed in going from an $L=16,20,24$ extrapolation to $L=20,24,28$ (an estimate of the systematic error) is given in parenthesis.

α	E_0/L	$\omega(k=0)=E_{\rm gap}$	$\omega(k=\pi/b)$	$E_B^{S=0}(k=0)$	$E_B^{S=0}(k=\pi/b)$	$E_B^{S=1}(k=\pi/b)$
0.0 [exact]	$-0.375=-3/8$	1	1	0	0	0
0.1	$-0.375\,480\,805$	0.946 279 339	1.051 248 884	0.0002	0.0456	0.0210
0.2	$-0.376\,974\,494$	0.885 209 996	1.104 980 718	0.0009(−2)	0.0824	0.0343
0.3	$-0.379\,566\,321$	0.816 844 275(+1)	1.161 143 536	0.0025(−1)	0.1104	0.0403
0.4	$-0.383\,356\,250$	0.741 061 41(+3)	1.219 628 893(+1)	0.0049(−3)	0.1294	0.0402
0.5	$-0.388\,465\,614$	0.657 477 7(+5)	1.280 237 618(+9)	0.0077(+34)	0.1394	0.0353
0.6	$-0.395\,048\,423(-3)$	0.565 296(+7)	1.3 426 173(+2)		0.1405	0.0280(+1)
0.7	$-0.40\,331\,243(-5)$	0.46 298(+5)	1.406 138(+3)		0.1327(−1)	0.0207(+17)
0.8	$-0.4\,135\,644(-8)$	0.3474(+3)	1.46 959(+4)		0.1151(−1)	
0.9	$-0.426\,330(-16)$	0.2098(+17)	1.5298(+8)		0.0829(+2)	
1.0	$-0.44\,314\,718\cdots$ $=1/4-\ln(2)$	0	1.5 707 963$\cdots$ $=\pi/2$		0	0

$$\frac{E_{\rm gap}}{J}=1-\frac{1}{2}\alpha-\frac{3}{2^3}\alpha^2+\frac{1}{2^5}\alpha^3-\frac{5}{2^7\times 3}\alpha^4-\frac{761}{2^{12}\times 3}\alpha^5 + \frac{(11)^2\times 157}{2^{16}\times 3^3}\alpha^6+\frac{21739}{2^{18}\times 3^3}\alpha^7-\frac{107\times 283\times 7079}{2^{24}\times 3^4\times 5}\alpha^8 + \frac{1307\times 9\,151\,183}{2^{28}\times 3^6\times 5^2}\alpha^9. \tag{29}$$

The zone-boundary ($k=\pi/b$) energy of the one-magnon state relative to E_0 to this order is

$$\frac{E_{\rm ZB}}{J}=1+\frac{1}{2}\alpha+\frac{1}{2^3}\alpha^2-\frac{1}{2^5\times 3}\alpha^4-\frac{83}{2^{12}\times 3}\alpha^5 - \frac{71\times 149}{2^{16}\times 3^3}\alpha^6-\frac{6373}{2^{14}\times 3^4}\alpha^7-\frac{19\times 128\,461}{2^{24}\times 3^2\times 5}\alpha^8 - \frac{41\times 256\,687\,901}{2^{28}\times 3^6\times 5^2}\alpha^9. \tag{30}$$

We can also use multiprecision methods to determine the one-magnon dispersion relation $\omega(k)$, parametrized by

$$\frac{\omega(k)}{J}=\sum_{l=0}^{\infty} a_l(\alpha)\cos(lkb). \tag{31}$$

On a finite lattice, momenta are only defined at the $N_d=L/2$ independent values of Eq. (3). [See also Fig. 1(b).] The relation $\omega(k)=\omega(-k)$ further reduces this to a total of $\mathrm{int}(N_d/2)+1$ independent lattice energies. These can be expanded as power series in α, and we again encounter finite lattice artifacts in these expansions beginning at $O(\alpha^{N_d})$.

The use of the lattice $\{\omega(k_n)\}$ to determine the Fourier coefficients in Eq. (31) is nontrivial because there are infinitely many coefficients but only $\mathrm{int}(N_d/2)+1$ lattice energies. We can proceed by determining the $\mathrm{int}(N_d/2)+1$ finite lattice Fourier coefficients $\{\hat{a}_l(\alpha,L)\}$, $l=0,1,\ldots,\mathrm{int}(N_d/2)$, defined by

$$\left.\frac{\omega(k_n)}{J}\right|_L=\sum_{l=0}^{\mathrm{int}(N_d/2)}\hat{a}_l(\alpha,L)\cos(lk_nb), \tag{32}$$

where $k_nb=2\pi n/N_d$.

We can invert this using a general result for the sum of a product of cosines over the discrete lattice momenta. We shall now assume N_d is even, so there are singly degenerate $k=0$ and $k=\pi/b$ points in addition to the doubly degenerate values $k=\pm 2\pi/N_db,\pm 4\pi/N_db,\ldots$. We can translate the $k=0$ and negative k values by $2\pi/b$, so a sum over lattice k values becomes a sum over $n=1,2,\ldots,N_d$, with $k_n=2\pi n/N_db$. The summed product of cosines is

$$\frac{1}{N_d}\sum_{l=1}^{N_d}\cos(2\pi ln/N_d)\cos(2\pi ln'/N_d) =\frac{1}{2}(\delta_{\mathrm{mod}(n-n',N_d),0}+\delta_{\mathrm{mod}(n+n',N_d),0}). \tag{33}$$

On multiplying Eq. (32) by $\cos(2\pi nl'/N_d)$ and summing over n, we therefore find the lattice Fourier coefficients

$$\hat{a}_l(\alpha,L)=\frac{2}{N_d}\frac{1}{(1+\delta_{l,0}+\delta_{l,N_d/2})}\times\sum_{n=1}^{N_d}\left.\frac{\omega(k_n)}{J}\right|_L\cos(2\pi ln/N_d). \tag{34}$$

If we assume more generally that the $\{\omega(k_n)\}$ are samplings of the continuous function given by Eq. (31), and invert the Fourier expansion using Eq. (33) we find

$$\frac{2}{N_d}\sum_{n=1}^{N_d}\left.\frac{\omega(k_n)}{J}\right|_L\cos(2\pi nl'/N_d) =\sum_{l=0}^{\infty}a_l(\delta_{\mathrm{mod}(l-l',N_d),0}+\delta_{\mathrm{mod}(l+l',N_d),0}). \tag{35}$$

As anticipated this constitutes $\mathrm{int}(N_d/2)+1$ constraints (the number of independent choices for l') on the infinite set of Fourier coefficients.

As an illustration, for $l'=0$ Eqs. (34) and (35) imply

$$\hat{a}_0=\frac{1}{N_d}\sum_{n=1}^{N_d}\left.\frac{\omega(k_n)}{J}\right|_L=\frac{1}{2}\sum_{l=0}^{\infty}a_l(\delta_{\mathrm{mod}(l,N_d),0}+\delta_{\mathrm{mod}(l,N_d),0}) =a_0+a_{N_d}+a_{2N_d}+\cdots. \tag{36}$$

Since we know that the perturbative series for both the lattice $\{\hat{a}_l\}$ and bulk-limit $\{a_l\}$ coefficients begin at $O(\alpha^l)$, the expansions of a_0 and $\hat{a}_0$ must be identical until we encounter contributions from higher-order coefficients; for a_0 these begin at $O(\alpha^{N_d})$ due to a_{N_d}. This is also the order at which finite-lattice artifacts appear in the energies, so there has been no loss of order reached in the a_0 expansion beyond the usual finite-lattice limitation. An equivalent conclusion follows for the Fourier coefficient $a_{N_d/2}$.

For the other Fourier modes the order of perturbation theory to which the bulk-limit coefficients are determined is reduced by the contributions of higher-order coefficients. For $l'=1$ for example we find

$$\hat{a}_1=\frac{2}{N_d}\sum_{n=1}^{N_d}\left.\frac{\omega(k_n)}{J}\right|_L\cdot\cos(2\pi n/N_d) =\sum_{l=0}^{\infty}a_l(\delta_{\mathrm{mod}(l-1,N_d),0}+\delta_{\mathrm{mod}(l+1,N_d),0}) =a_1+a_{N_d+1}+a_{2N_d+1}+\cdots+a_{N_d-1}+a_{2N_d-1}+\cdots. \tag{37}$$

The contributions of the two delta functions that combined in the previous $l'=0$ example are now distinct, so there is an $O(\alpha^{N_d-1})$ difference due to a_{N_d-1} between the known lattice series for $\hat{a}_1$ and the bulk-limit a_1 series. The worst case is $m'=N_d/2-1$; the lattice and bulk-limit coefficients are then related by

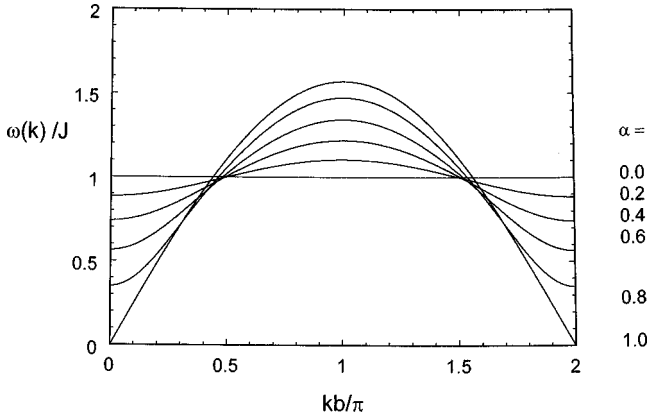

FIG. 4. Dispersion $\omega(k)$ of the one-magnon band in the alternating chain for $\alpha=0.2$, 0.4, 0.6, 0.8, and 1.0, using the fifth-order dispersion relation Eqs. (31),(39). The $\alpha=1$ curve is the exact result $\pi|\sin(kb/2)|/2$.

$$\hat{a}_{N_d/2-1}=a_{N_d/2-1}+a_{3N_d/2-1}+\cdots+a_{N_d/2+1}+a_{3N_d/2+1}+\cdots, \tag{38}$$

so the series for the bulk-limit $a_{N_d/2-1}$, which begins at $O(\alpha^{N_d/2-1})$, cannot be determined beyond $O(\alpha^{N_d/2})$ due to the presence of $a_{N_d/2+1}$. Thus we conclude that the perturbative expansion of the bulk-limit dispersion relation Eq. (31) can only be *completely* determined to $O(\alpha^{N_d/2})$ from finite lattice data. The attainable order depends on the mode, and is in general $O(\alpha^{N_d-1-\mathrm{mod}(l,N_d/2)})$ for a_l with $N_d/2\geq l\geq 0$.

It follows that the complete set of bulk-limit Fourier coefficients $\{a_l\}$ is uniquely determined just to $O(\alpha^5)$ by the diagonalization of the $L=20$ lattice. These coefficients, which confirm and continue the one-magnon dispersion relation of Brooks Harris, Eq. (16), are

$$\begin{aligned}
a_0&=1 &&-\frac{1}{16}\alpha^2+\frac{3}{64}\alpha^3+\frac{23}{1024}\alpha^4-\frac{3}{256}\alpha^5,\\
a_1&= &&-\frac{1}{2}\alpha-\frac{1}{4}\alpha^2+\frac{1}{32}\alpha^3+\frac{5}{256}\alpha^4-\frac{35}{2048}\alpha^5,\\
a_2&= &&-\frac{1}{16}\alpha^2-\frac{1}{32}\alpha^3-\frac{15}{512}\alpha^4-\frac{283}{18432}\alpha^5,\\
a_3&= &&-\frac{1}{64}\alpha^3-\frac{1}{48}\alpha^4-\frac{9}{1024}\alpha^5,\\
a_4&= &&-\frac{5}{1024}\alpha^4-\frac{67}{9216}\alpha^5,\\
a_5&= &&-\frac{7}{4096}\alpha^5.
\end{aligned} \tag{39}$$

The fifth-order one-magnon dispersion relation given by Eqs. (31),(39) is shown for a range of alternations in Fig. 4.

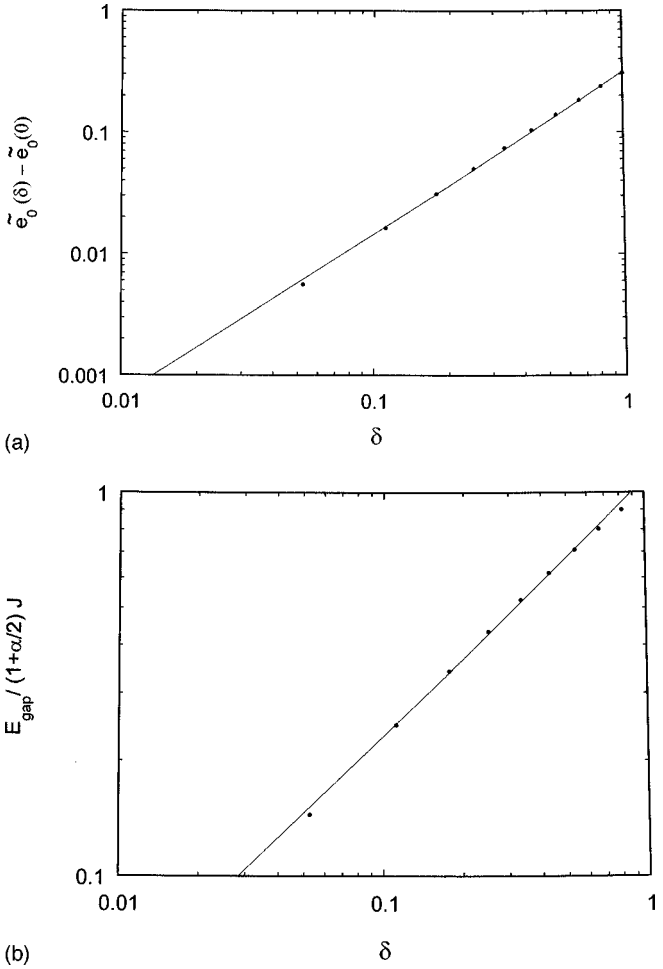

FIG. 5. Critical behavior of the alternating chain as a function of δ, with $\mathcal{J}$ fixed. (a) shows the energy per spin relative to the bulk limit, $\tilde{e}_0(\delta)-\tilde{e}_0(0)$, and a fit to $c_1\delta^{4/3}$ which gives $c_1=0.3134$. (b) shows $E_{\mathrm{gap}}/\mathcal{J}$ and a fit to $c_1\delta^{3/4}$ which gives $c_1=2.003$.

C. Numerical results versus predicted critical behavior

The expected behaviors of $E_{\mathrm{gap}}/\mathcal{J}$ and $\tilde{e}_0(\delta)=E_0/\mathcal{J}L=2e_0(\alpha)/(1+\alpha)$ as we approach the critical point $\delta=0$ are[11,12]

$$\lim_{\delta\to 0}\tilde{e}_0(\delta)-\tilde{e}_0(\delta=0)\propto\frac{\delta^{4/3}}{|\ln\delta|} \tag{40}$$

and

$$\lim_{\delta\to 0}\frac{E_{\mathrm{gap}}}{\mathcal{J}}\propto\frac{\delta^{2/3}}{|\ln\delta|^{1/2}}. \tag{41}$$

As we have no information regarding the range of validity of these predicted asymptotic forms, it is of great interest to test their accuracy for values of δ realized in nature, for example in $(VO)_2P_2O_7$, with $\delta\approx 0.1$.

We will now compare these theoretical asymptotic forms with our numerical results for $E_{\rm gap}/\mathcal{J}$ and $\tilde{e}_0(\delta)$ at small δ. Taking the ground state energy per spin first, in Fig. 5(a) we show a logarithmic plot of $\tilde{e}_0$ versus δ; evidently the smaller δ values do support approximate power-law behavior in the range we have studied. A fit of the three smallest-δ points to the form $c_1\delta^p$ gives $c_1=0.3632$ and $p=1.412$, apparently consistent with $\delta^{4/3}$ times logarithmic corrections. The anticipated theoretical form $c_1\delta^{4/3}/|\ln\delta|$, however, does not give an especially good fit, and is actually worse than a pure 4/3 power law. A 4/3 power fit to the three smallest δ points gives $c_1=0.3134$, which is reasonably accurate for larger δ as well; this fit is shown in Fig. 5(a).

The δ dependence we observe for the singlet-triplet gap scaled by $\mathcal{J}$ is shown in Fig. 5(b). The approximate linearity of the log-log plot suggests power-law behavior over the full range of δ considered. A fit of all points to $c_1\delta^p$ gives $c_1=1.999$ and $p=0.7497$, which favors a power law fit with $\delta^{3/4}$ rather than the theoretical $\delta^{2/3}$ of Eq. (41). Fitting $c_1\delta^{3/4}$ to the three smallest δ points gives $c_1=2.003$, which is shown in Fig. 5(b). Evidently this is a remarkably good fit. The surprising accuracy of this form for large alternation can be understood by noting that the similar function $E_{\rm gap}/\mathcal{J}=2\delta^{3/4}$, corresponding to $E_{\rm gap}/J=(1-\alpha)^{3/4}(1+\alpha)^{1/4}$, gives the correct $E_{\rm gap}/J$ power series Eq. (17) to $O(\alpha^2)$.

The form $c_1\delta^{2/3}/|\ln\delta|^{1/2}$ found by Black and Emery gives a less accurate description of our data. Thus we appear to support a different asymptotic power law than expected for the singlet-triplet gap, although we cannot continue to very small δ to see the range over which this discrepancy persists.

Thus we conclude that the predicted critical behavior for small δ gives a rather inaccurate description of the ground-state energy and singlet-triplet gap for values of δ typical of real materials, which implies that these formulas are unfortunately of little utility for experimentalists. Simple generalizations of the theoretical critical forms do, however, give useful parametrizations of these energies for the range of δ we have considered.

In view of the inaccuracies we have found, the behavior of the ground state energy and gap much closer to the critical point would be an interesting topic for a detailed investigation on large lattices, using a finite-size scaling analysis. The energies on very large lattices might be obtained using the DMRG approach.[26]

VI. TWO-MAGNON BOUND STATES

Recent theoretical work[15,17–19] motivated by neutron scattering studies of $CuGeO_3$[3] has led to considerable interest in two-magnon bound states in dimerized quantum spin systems. The existence of such bound states in the alternating chain model appears very likely, since the interdimer interaction H_I, Eq. (5), gives an attractive diagonal potential energy between two adjacent excited dimers if their total spin is $S=0$ or $S=1$. To see this, note the effect of H_I on a state of adjacent $(+)(0)$ dimer excitons

$$
\begin{aligned}
H_I|\circ(+)(0)\circ\rangle = \frac{\alpha J}{4}\Big\{ & \underbrace{|\circ(0)(+)\circ\rangle}_{\text{transpose}} \\
& \underbrace{-|(+)\circ(0)\circ\rangle - |\circ(+)\circ(0)\rangle}_{\text{hop}} \\
& \underbrace{+|\circ(+)\circ\circ\rangle + |\circ\circ(+)\circ\rangle}_{\text{deexcite}} \\
& \underbrace{+|(+)(0)(0)\circ\rangle - |(0)(+)(0)\circ\rangle}_{\text{excite}} \\
& \underbrace{+|\circ(+)(+)(-)\rangle - |\circ(+)(-)(+)\rangle}_{\text{excite}} \\
& +\sqrt{3}\sum_{m'=1}^{N_d}{}' \underbrace{|(0,0)_{m',m'+1}\cdots(+)(0)\cdots\rangle}_{\text{double excite}}\Big\}\,.
\end{aligned}
\tag{42}
$$

Again in Σ' the index m' takes on all values that do not superimpose a dimer excitation on the already excited $(+)$ or $(-)$ sites.

The analogous expressions for other polarization states may be combined to give the effect of H_I on nearest neighbor dimer excitons with definite total spin. There is a diagonal interaction due to the ''transpose'' matrix element and others that retain two neighboring excitons. This static inter-exciton potential is

$$
\langle (S,S_z)_{m,m+1}|H_I|(S,S_z)_{m,m+1}\rangle = \begin{cases} +J\alpha/4 & S=2, \\ -J\alpha/4 & S=1, \\ -J\alpha/2 & S=0. \end{cases} \tag{43}
$$

This suggests that at large alternation (small α) we should find two-magnon bound states with $S=0$ and $S=1$, with binding energies of approximately $J\alpha/2$ and $J\alpha/4$, respectively. (This only applies to $k=\pi/b$; at other k values there is a complication that modifies this result, as noted below.)

We can again use numerical results with small coupling α to establish the higher-order perturbation series for properties of these bound states. Unfortunately this is a much more difficult numerical problem than the study of the ground state and one-magnon levels, so here we give only a few preliminary results.

The binding energies E_B of the $S=0$ and $S=1$ bound states are defined by

$$
E_B(k) = \min_{k_1+k_2=k}\,[\omega(k_1)+\omega(k_2)] - [E(k)-E_0]. \tag{44}
$$

(The ω sum gives the onset of the two-magnon continuum at k.) Assuming that the continuum onset at $k=\pi/b$ is given by $k_1=0$ and $k_2=\pi/b$, we find that the two-magnon binding energies to $O(\alpha^2)$ on $L\geqslant 12$ lattices are

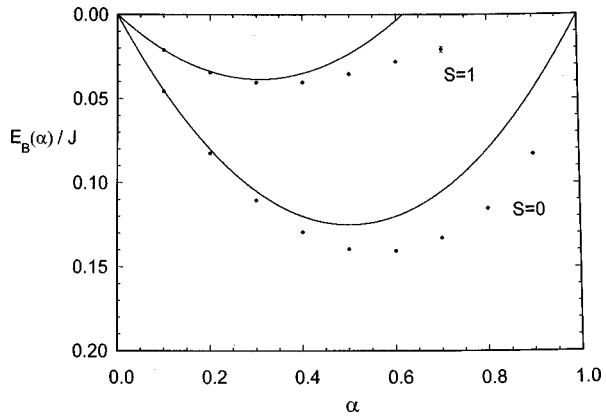

FIG. 6. Binding energies of the $S=0$ and $S=1$ two-magnon bound states at $k=\pi/b$ (band maximum). The points are bulk-limit extrapolations of Lanczos data (Table II) and the lines are second order perturbation theory, Eq. (45).

$$\frac{E_B(k=\pi/b)}{J}=\begin{cases}\frac{1}{4}\alpha-\frac{13}{32}\alpha^2 & S=1,\\ \frac{1}{2}\alpha-\frac{7}{16}\alpha^2 & S=0.\end{cases} \tag{45}$$

Our numerical result for the bulk-limit binding energies at $k=\pi/b$ (Table II and Fig. 6) are clearly consistent with these perturbative results at small α. It is interesting that the binding is much weaker near $k=0$, for example the expansion of the $S=0$ binding energy at $k=0$ appears to begin at $O(\alpha^2)$.

The determination of these perturbative binding energies analytically at general k is a complicated problem because the two-exciton sector is a manifold of degenerate states under H_0. Determining the appropriate basis states within this degenerate manifold requires diagonalization of the ''hopping'' part of H_I. This is only straightforward at $k=\pi/b$, where this hopping amplitude vanishes; as an illustration, for adjacent $(+)(0)$ excitons we find

$$\langle(+)\circ(0)\circ;k|H_I|\circ(+)(0)\circ;k\rangle\propto\cos(kb/2). \tag{46}$$

Thus $k=\pi/b$ bound states do not mix with the two-exciton continuum to leading order, and remain relatively localized.

Except near $k=\pi/b$ we expect the coupling between nearest-neighbor and separated excitons to be very important, because the energy denominator is $O(\alpha J)$, which is the same order as the hopping matrix element. This implies that there are corrections to the bound-state wave function of order $O(\langle H_I\rangle/\Delta E)=O(\alpha J)/O(\alpha J)=O(\alpha^0)$ and corrections to the static binding energy Eq. (43) of order $O(|\langle H_I\rangle|^2/\Delta E)=O(\alpha)$ except at $k=\pi/b$.

This degenerate two-exciton perturbation problem has been solved at leading order by Uhrig and Schulz[15] and by Damle and Nagler[16] for the $S=1$ two-magnon bound state, with the result

$$\frac{E_B(k)}{J}=\alpha\left(\frac{1}{4}+\cos(kb/2)[\cos(kb/2)-1]\right), \tag{47}$$

with solutions only over the range $|\pi-kb|\leq\pi/3$. The most deeply bound two-magnon state, at $k=\pi/b$, has $E_B=\alpha/4$ to leading order, consistent with our $S=1$ result Eq. (45).

At the extreme point $k=0$ we see no evidence for an $S=1$ bound state in our numerical extrapolation of Lanczos data. Although we do see evidence of an $S=0$ bound state at $k=0$, it is quite weakly bound and (in consequence) has a very extended spatial wave function. The difference between $k=0$ and $k=\pi/b$ bound state wave functions was quite evident in the finite-size effects seen in our numerical extrapolation.

In a preliminary numerical study of a truncated system of zero-, one- and two-exciton states on an $L=200$ lattice we find that the attractive potentials in Eq. (43) are strong enough to form an $S=0$ bound state for all k, but apparently the $S=1$ bound state exists only for a range of k around π/b. Similar conclusions have been reported by Uhrig and Schulz[15] and Bouzerar *et al.*[17]

These results are especially relevant to the alternating-chain material $(VO)_2P_2O_7$, (VOPO). An excitation has been observed in VOPO just below the two-magnon continuum, which has been cited as a possible two-magnon bound state.[4,5] Since this peak is seen clearly for a range of k including $k\approx 2\pi/b$ (equivalent to the $k=0$ point where we find no $S=1$ bound state), it is inconsistent with the expectations of the alternating chain model for such a bound state. If mode observed in VOPO is indeed a two-magnon bound state, its persistence to $k\approx 2\pi/b$ is presumably due to additional interactions.

VII. NEUTRON SCATTERING STRUCTURE FACTOR

A. General results

Identification of the magnetic excitations predicted by the alternating chain model will be facilitated by estimates of their couplings to external probes, such as photons (especially for $S=0$ states, through Raman scattering) and neutrons (for $S=1$ states). Here we present perturbative and numerical results for the neutron scattering structure factor to the one-magnon mode.

The neutron scattering cross section is proportional to the structure factor, which in the Heisenberg picture is

$$S_{mm'}(\vec{k},\omega)=\frac{1}{2\pi}\int_{-\infty}^{\infty}dt\,e^{i\omega t}e^{i\vec{k}\cdot(\vec{x}_i-\vec{x}_j)}\times\sum_{\text{sites }i,j}\langle\psi_0|S_m^{\dagger}(\vec{x}_j,t)S_{m'}(\vec{x}_i,0)|\psi_0\rangle. \tag{48}$$

We can insert a complete set of eigenstates $\{|\psi_N\rangle\}$ of the full H between the spins in this matrix element and write the spin structure factor as a sum over *exclusive structure factors*

$$S_{mm'}(\vec{k},\omega)=\sum_N S_{mm'}^{\psi_0\to\psi_N}(\vec{k},\omega), \tag{49}$$

where

$$S^{\psi_0\to\psi_N}_{mm'}(\vec{k},\omega)=\sum_{\text{sites } i,j}\frac{1}{2\pi}\int_{-\infty}^{\infty}dt\, e^{i\omega t}e^{i\vec{k}\cdot(\vec{x}_i-\vec{x}_j)} \times\langle\psi_0|S^{\dagger}_m(\vec{x}_j,t)|\psi_N\rangle\langle\psi_N|S_{m'}(\vec{x}_i,0)|\psi_0\rangle. \tag{50}$$

Each exclusive structure factor $S^{\psi_0\to\psi_N}_{mm'}(\vec{k},\omega)$, gives the intensity of scattering from $|\psi_0\rangle$ to a specific excited state $|\psi_N\rangle$.

The Heisenberg picture operator $S^{\dagger}_m(\vec{x}_j,t)=\exp(iHt)S^{\dagger}_m(\vec{x}_j,0)\exp(-iHt)$ gives trivial exponentials in t, so the time integral leads to a single energy-conserving delta function. In isotropic antiferromagnets the ground state typically has $S=0$, so the accessible excited states $\{|\psi_N\rangle\}$ all have $S=1$. We can then evaluate this exclusive structure factor to a specific polarization state, here $S_z=+1$, without loss of generality. For $S_z=+1$ the only nonzero spherical component of the exclusive structure factor is then

$$S^{\psi_0\to\psi_N}_{++}(\vec{k},\omega)=\delta(E_N-E_0-\omega)\Big|\sum_i\langle\psi_N|S_+(\vec{x}_i)|\psi_0\rangle e^{i\vec{k}\cdot\vec{x}_i}\Big|^2. \tag{51}$$

If the excited state $|\psi_N\rangle$ is an eigenstate of momentum, which we can assume for the alternating chain again without loss of generality, the matrix elements of the spin operator at translationally equivalent sites are equal modulo a plane wave

$$\langle\psi_N(\vec{p})|S_m(\vec{x}_i)|\psi_0\rangle=e^{-i\vec{p}(\vec{x}_i-\vec{x}_0)}\langle\psi_N(\vec{p})|S_m(\vec{x}_0)|\psi_0\rangle, \tag{52}$$

where $\vec{x}_0$ is some reference site. The sum over all spin sites i can then be reduced to a sum over all sites in the unit cell $i*$ times a momentum conserving delta function

$$S^{\psi_0\to\psi_N}_{++}(\vec{k},\omega)=N^2_{\text{unit cells}}\delta(E_N-E_0-\omega)\,\delta_{\vec{k},\vec{p}}\cdot \times\left|\sum_{\substack{\text{sites } i*\text{in}\\ \text{unit cell}}}\langle\psi_N(\vec{p})|S_+(\vec{x}_{i*})|\psi_0\rangle e^{i\vec{k}\cdot\vec{x}_{i*}}\right|^2. \tag{53}$$

If we are only interested in the k dependence and *relative* intensities of neutron scattering from the various $S=1$ excitations, the overall normalization is irrelevant, and we can simply evaluate dimensionless reduced intensities. It is convenient to normalize this reduced exclusive structure factor as

$$\mathcal{S}(\vec{k})=N_{\text{unit cells}}\left|\sum_{i*}\langle\psi_N(\vec{k})|S_+(\vec{x}_{i*})|\psi_0\rangle e^{i\vec{k}\cdot\vec{x}_{i*}}\right|^2. \tag{54}$$

(Here and for the remainder of the paper we suppress the superscript $\psi_0\to\psi_N$ and spin indices on the exclusive structure factor.) This expression can be evaluated analytically (using perturbation theory or other approximate wave functions) or numerically using wave functions on finite lattices.

B. One-magnon exclusive S(k)

We will now consider the reduced exclusive neutron scattering structure factor $S(k)$, Eq. (54), for the excitation of one-magnon states in the alternating chain, using dimer perturbation theory and the multiprecision technique. The exclusive structure factor involves the matrix element

$$\sum_{i*=1,2}\langle\psi_N(\vec{k})|S_+(\vec{x}_{i*})|\psi_0\rangle e^{i\vec{k}\cdot\vec{x}_{i*}} =\langle\psi_1(k)|(S^L_+e^{-ikd/2}+S^R_+e^{+ikd/2})|\psi_0\rangle. \tag{55}$$

The superscripts L and R refer to the left and right spins in the first dimer. Note that this can be written as a sum of dimer-spin conserving and changing terms

$$S^L_+\,e^{-ikd/2}+S^R_+\,e^{+ikd/2} =\cos(kd/2)\ \underbrace{\left(S^L_++S^R_+\right)}_{\text{dimer-spin conserving}} +\sin(kd/2)\ \underbrace{\frac{1}{i}\left(S^L_+-S^R_+\right)}_{\text{dimer-spin changing}}. \tag{56}$$

For the one-magnon excitation it suffices to determine the matrix element of the raising operator on a single spin, because S^L_+ and S^R_+ have opposite one-magnon matrix elements for any k. (This is not true for a general $S=1$ excitation.) Evaluating the matrix element of S^L_+ to $O(\alpha)$ using the perturbative $|\psi_0\rangle$ and $|\psi_1(k)\rangle$, Eq. (12) and Eq. (15), we find

$$\langle\psi_1(k)|S^L_+|\psi_0\rangle=-\frac{1}{\sqrt{L}}\left(1+\frac{\alpha}{4}\cos(kb)\right) \tag{57}$$

so the matrix element Eq. (55) is

$$\sum_{i*=1,2}\langle\psi_N(\vec{k})|S_+(\vec{x}_{i*})|\psi_0\rangle e^{i\vec{k}\cdot\vec{x}_{i*}} =\frac{1}{\sqrt{L}}(e^{ikd/2}-e^{-ikd/2})\left(1+\frac{\alpha}{4}\cos(kb)\right). \tag{58}$$

The one-magnon exclusive neutron scattering structure factor $S(k)$ is proportional to the modulus squared of this spin matrix element. To $O(\alpha)$ we find

$$\mathcal{S}(k)=(1-\cos(kd))\left(1+\frac{\alpha}{2}\cos(kb)\right). \tag{59}$$

The small-k suppression $1-\cos(kd)\propto\sin(kd/2)^2$ is familiar from isolated dimer problems and gives a basic intensity ''envelope'' that measures the dimer size d. (See, for example, Ref. 27.) The separation *between* dimer centers b enters as a more rapid modulation $1+(\alpha/2)\cos(kb)$ of the intrinsic dimer form $1-\cos(kd)$. This $O(\alpha)$ modulation arises from the excitation of the ''two-exciton'' component of the ground state $|\psi_0\rangle$ to the unperturbed ''one-exciton'' compo-

nent of $|\psi_1(k)\rangle$, and apparently has been observed in recent neutron scattering experiments on single crystals of $Sr_{14}Cu_{24}O_{41}$.[28]

The $\mathcal{S}(k)$ series Eq. (59) may be continued using the multiprecision approach. We introduce a cosine expansion for the S_+^L matrix element

$$\langle\psi_1(k)|S_+^L|\psi_0\rangle=-\frac{1}{\sqrt{L}}\sum_{l=0}^{\infty}s_l(\alpha)\cos(lkb) \tag{60}$$

and the coefficients we find to $O(\alpha^3)$ are

$$\begin{aligned} s_0&= 1-\frac{11}{64}\alpha^2-\frac{5}{128}\alpha^3,\\ s_1&= +\frac{1}{4}\alpha-\frac{1}{16}\alpha^2+\frac{31}{1536}\alpha^3,\\ s_2&= +\frac{5}{64}\alpha^2+\frac{31}{384}\alpha^3,\\ s_3&= +\frac{15}{512}\alpha^3. \end{aligned} \tag{61}$$

These have the same order finite size effects as the dispersion Fourier coefficients $\{a_l\}$, so diagonalization of an L site chain gives the complete set of exclusive structure factor Fourier coefficients to $O(\alpha^{L/4})$.

These coefficients determine the $O(\alpha^3)$ generalization of Eq. (59), which is

$$\begin{aligned} \mathcal{S}(k)=&(1-\cos(kd))\cdot\\ &\left\{\left(1-\frac{5}{16}\alpha^2-\frac{3}{32}\alpha^3\right)+\left(\frac{1}{2}\alpha-\frac{1}{8}\alpha^2-\frac{5}{192}\alpha^3\right)\cos(kb)\right.\\ &\left.+\left(\frac{3}{16}\alpha^2+\frac{7}{48}\alpha^3\right)\cos(2kb)+\frac{5}{64}\alpha^3\cos(3kb)\right\}. \end{aligned} \tag{62}$$

A numerical example of this exclusive structure factor is presented in Fig. 8 for the case of $(VO)_2P_2O_7$, which will be discussed in Sec.VIII.

C. Two-magnon bound state exclusive S(k)

To evaluate the exclusive neutron scattering structure factor to the $S=1$ two-magnon bound state we require the spin matrix element Eq. (55). This bound state is excited by a rather different mechanism than the one-magnon state discussed in Sec. VII B above. To leading order the bound state wave function is

$$|\psi_1^{(0)}(k)\rangle=\frac{1}{\sqrt{N_d}}\sum_{m=1}^{N_d}e^{ikx_m}|(1,1)_{m,m+1}\rangle \tag{63}$$

which is invisible to neutron excitation of the ''bare'' ground state, since two spin flips are required to connect these states.

At $O(\alpha)$ a coupling to neutrons appears through the nonleading parts of the ground state and bound state. There are two such contributions, which are apparent on inspecting the $O(\alpha)$ states

$$|\psi_0\rangle=|0\rangle-\frac{\sqrt{3}}{8}\alpha\sum_{m=1}^{N_d}|(0,0)_{m,m+1}\rangle \tag{64}$$

and

$$\begin{aligned} |\psi_1(k)\rangle=\frac{1}{\sqrt{N_d}}\sum_{m=1}^{N_d}e^{ikx_m}\Big[&|(1,1)_{m,m+1}\rangle\\ &+O(\alpha^0)|(1,1)_{m,n}\rangle\text{terms, with }|m-n|\geqslant 2\\ &+\frac{\alpha}{2\sqrt{2}}(1+e^{-ikb})|(+)_m\rangle+\cdots\Big]. \end{aligned} \tag{65}$$

In the matrix element $\langle\psi_1(k)|S_+(x)|\psi_0\rangle$there is a $0\rightarrow 1$ exciton coupling of the bare ground state to the $O(\alpha)$ one-exciton component of the perturbed bound state, which has the same form as the leading one-magnon matrix element. The second contribution is the $2\rightarrow 2$ exciton coupling of the $O(\alpha)|(0,0)\rangle$ two-exciton part of the ground state to the two-exciton bare bound state.

These matrix elements have quite different k dependences because the $0\rightarrow 1$ term is dimer-spin changing and the $2\rightarrow 2$ term is dimer-spin conserving. From Eq. (56) one can see that this leads to prefactors of $\sin(kd/2)$ and $\cos(kd/2)$, respectively. Since the one-magnon $S(k)$ has an overall $\sin(kd/2)$ dependence, it may be possible to distinguish one-magnon and bound state modes by this k dependence.

The reduced structure factor $\mathcal{S}(k)$ for the $S=1$ two-magnon bound state has been derived to leading order by Damle and Nagler,[16] with the result (in our conventions)

$$\mathcal{S}(k)=\frac{\alpha^2}{4}[1-4\cos^2(kb/2)]\sin^2[k(b-d)/2]. \tag{66}$$

This does indeed show characteristic dependence on d and b that could be used as an experimental signature.

We unfortunately encountered difficulties in numerical studies of the bound state. We found very slow convergence of our projection method to this state, perhaps due to the presence of a nearby bulk-limit continuum, so the use of our multiprecision techniques was not practical. This method requires implementation of an alternative iteration scheme with better convergence. Work along these lines is in progress; we plan to present results for bound state energies and matrix elements in a future publication.

VIII. COMPARISON WITH $(VO)_2P_2O_7$

To illustrate the utility of our results we will now apply them to the one-magnon dispersion relation $\omega(k)$ and exclusive neutron scattering intensity $\mathcal{S}(k)$ observed in $(VO)_2P_2O_7$. This material is an alternating chain with magnetic V^{4+} ion spacings of 3.2 Å and 5.1 Å along the chain pathways.[4] The chains run along the crystallographic b direction, and there is a weaker interchain coupling J_a along the ''ladder'' direction a, which gives a leading-order contribution of $J_a\cos(k_a)$ to $\omega(k)$.

A fit of the low-lying one-magnon branch $\omega([0,k_b=k,0])$ observed in VOPO to the fifth order formula Eqs.

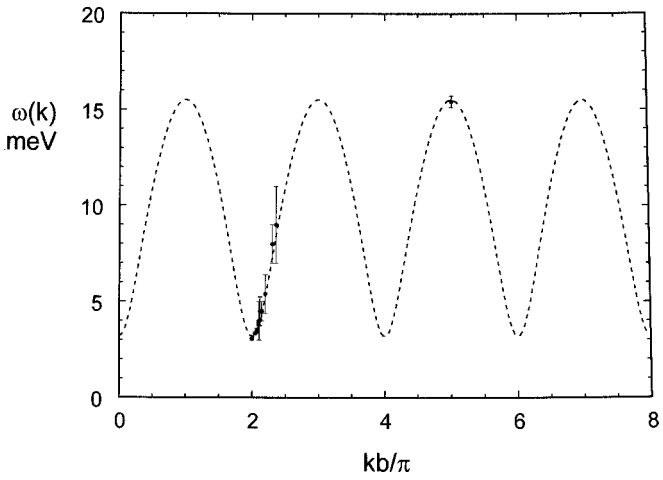

FIG. 7. A fit of the alternating chain dispersion relation Eqs. (31),(39) to the one-magnon dispersion observed in neutron scattering from $(VO)_2P_2O_7$ (Ref. 4), as discussed in Sec. VIII. The fitted parameters are $J=11.0$ meV and $\alpha=0.796$.

(31),(39) is shown in Fig. 7. (Since VOPO has $J_a\approx-0.73$ meV we have added this J_a to the theoretical result Eq. (31) to obtain $\omega[k_a=0,k_b=k,k_c=0]$.) A least-squares fit gives an exchange of $J=11.0(1)$ meV and alternation of $\alpha=0.796(4)$, which provides an excellent account of the data. We can similarly fit the more accurate ninth-order formulas for $E_{\rm gap}$ and $E_{\rm ZB}$ [Eqs. (29),(30)], including the J_a shift, to the measured values of 3.1(1) meV and 15.4(3) meV; this gives consistent values of $J=10.92$ meV and $\alpha=0.798$.

The intensity of the modes seen in neutron scattering is quite sensitive to the spatial geometry of the alternating chain. For VOPO we can use this relation to deduce which is the stronger of the two inequivalent exchange paths in the chain. Figure 8 shows the theoretical one-magnon intensity variation over a wide range of k. The dashed line is the $[1-\cos(kd)]$ scattering intensity for isolated dimers, and the solid line shows the $O(\alpha^3)$ alternating-chain result Eq. (55) for $\mathcal{S}(k)$, with $\alpha=0.8$ and $d/b=5.1$ Å/8.3 Å. This d/b ratio assumes that the long V-PO_4-V dimer, which has $d=5.1$ Å, has the stronger interaction J. The characteristic variation of $\mathcal{S}(k)$, which is measured in neutron scattering, allows a direct check of this bond assignment and is a stringent test of the alternating chain model as applied to VOPO (Ref. 34, in preparation).

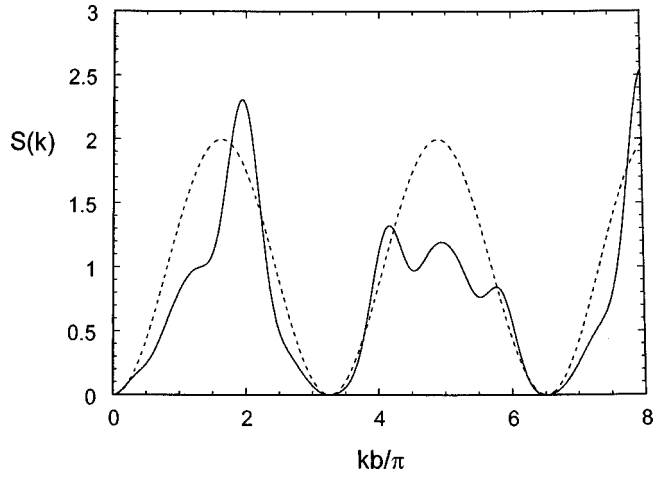

FIG. 8. The predicted neutron scattering intensity (exclusive structure factor) $\mathcal{S}(k)$ for the one-magnon mode in $(VO)_2P_2O_7$, Eq. (62). The parameters are $\alpha=0.8$ (from a fit to the dispersion), $d=5.1$ Å and $b=8.3$ Å. The dashed line shows the isolated dimer form $[1-\cos(kd)]$ for comparison.

IX. SUMMARY AND CONCLUSIONS

In summary, we have presented many new analytical and numerical results for the low-lying excitations of the spin-1/2 alternating Heisenberg chain. We introduced the model in Secs. I and II, and Sec. III reviewed previous work. Section IV A introduced perturbation theory about the dimer limit, and in Sec. IV B we used this approach to confirm previous results for the one-magnon dispersion $\omega(k)$ to third order, and extended the ground state energy calculations to fourth order. Section IV C summarized the expected critical behavior of the gap and ground-state energy as we approach the uniform chain limit. Relations between energies and their derivatives at the critical point were also derived. To complement these analytical calculations, in Sec. V A we undertook numerical calculations of bulk limit energies of the ground state, gap, zone boundary, and $S=0$ and $S=1$ two magnon bound states, using Lanczos methods on systems up to $L=28$. As a major part of this work, in Sec. V B we introduced a technique in which multiple precision calculations with a very small dimer coupling are used to infer perturbation expansions to high order. This confirmed third and fourth order energy expansions and allowed continuation of the e_0, $E_{\rm gap}$, and $E_{\rm ZB}$ series to $O(\alpha^9)$. The one-magnon dispersion relation $\omega(k)$ was then derived to $O(\alpha^5)$ using this method. The expected critical behavior of the ground state energy and energy gap was compared with our numerical results in Sec. V C. The ground state energy was found to be in approximate agreement with the expected (to within logarithmic corrections) $\delta^{4/3}$ power law. The singlet-triplet gap however appears to support a power law of $\delta^{3/4}$ rather than $\delta^{2/3}$ over the accessible range of δ. Section VI considered two-magnon bound states. At the zone boundary $k=\pi/b$ an attractive potential between magnons was found to give rise to $S=0$ and $S=1$ two-magnon bound states for all alternations. Numerical results and $O(\alpha^2)$ analytical forms were given for the magnon-magnon binding energy. The $S=0$ bound state was found for all k considered, and numerical results for its binding energy at $k=0$ were also given. The $S=1$ bound state however was found to exist only for a range of k near π/b. In Sec. VII we introduced an exclusive neutron scattering structure factor $\mathcal{S}(k)$; this was evaluated analytically for the one-magnon band using the multiple precision technique and dimer perturbation theory. The one-magnon exclusive structure factor was determined to $O(\alpha^3)$, and was presented as a modulation times the familiar isolated-dimer form $[1-\cos(kd)]$. Finally, in Sec. VIII we gave an illustrative application of these results to recent neutron scattering data on $(VO)_2P_2O_7$, which is dominantly an alternating chain. We showed that the fifth-order dispersion relation gives an excellent fit to the observed one-magnon band, and noted that the predicted exclusive structure factor $\mathcal{S}(k)$ will allow a detailed test of the alternating chain model as applied to $(VO)_2P_2O_7$.

In conclusion, we have used perturbation theory and numerical methods to calculate the properties of the ground state and one- and two-magnon states in the alternating Heisenberg chain. Using a technique based on multiple precision programming we have derived high-order series expansions for energies and matrix elements of the alternating chain. This technique is quite general and should be applicable to many other quasi-1D quantum spin systems.

ACKNOWLEDGMENTS

We acknowledge useful discussions with D. Bailey, E. Dagotto, K. Damle, R.S. Eccleston, V. Emery, A.W. Garrett, S.E. Nagler, D.J. Scalapino, H.J. Schulz, and P.D.Stevenson. This work was supported in part by the United States Department of Energy under Contract No. DE-AC05-96OR22464 at the Oak Ridge National Laboratory, managed for the U.S. DOE by Lockheed Martin Energy Research Corporation.

[1] For early work in this area see P.L. Nordio, Z.G. Soos, and H.M. McConnell, Annu. Rev. Phys. Chem. **17**, 237 (1966).

[2] M. Nishi, O. Fujita, and J. Akimitsu, Phys. Rev. B **50**, 6508 (1994).

[3] M. Aïn, J. E. Lorenzo, L. P. Regnault, G. Dhalenne, A. Revcolevschi, B. Hennion, and Th. Jolicoeur, Phys. Rev. Lett. **78**, 1560 (1997).

[4] A.W. Garrett, S.E. Nagler, D.A. Tennant, B.C. Sales, and T. Barnes, Phys. Rev. Lett. **79**, 745 (1997).

[5] A.W. Garrett, S.E. Nagler, T. Barnes, and B.C. Sales, Phys. Rev. B **55**, 3631 (1997).

[6] W. Duffy and K.P. Barr, Phys. Rev. **165**, 647 (1968).

[7] J. Bonner and H.W.J. Blöte, Phys. Rev. B **25**, 6959 (1982).

[8] M. Kohmoto, M. den Nijs, and L.P. Kadanoff, Phys. Rev. B **24**, 5229 (1981); M. Yamanaka, Y. Hatsugai, and M. Kohmoto, *ibid.* **48**, 9555 (1993); **50**, 559 (1994). These use the method of M.P. Gelfand, R.R.P. Singh, and D.A. Huse (Ref. 9). It is possible to extend this coupled cluster approach to excitations, as noted by M.P. Gelfand, Solid State Commun. **98**, 11 (1996); for applications to related spin systems, see J. Oitmaa, R.R.P. Singh, and Z. Weihong, Phys. Rev. B **54**, 1009 (1996); Z. Weihong, *ibid.* **55**, 12 267 (1997).

[9] M.P. Gelfand, R.R.P. Singh, and D.A. Huse, J. Stat. Phys. ; **59**, 1093 (1990), see Table IV, p. 1135 for the e_0 series.

[10] M.P.M. den Nijs, Physica A **95**, 449 (1979).

[11] M.C. Cross and D. Fisher, Phys. Rev. B **19**, 402 (1979).

[12] J.L. Black and V.J. Emery, Phys. Rev. B **23**, 429 (1981).

[13] Z.G. Soos, S. Kuwajima, and J.E. Mihalick, Phys. Rev. B **32**, 3124 (1985).

[14] G. Spronken, B. Fourcade, and Y. Lépine, Phys. Rev. B **33**, 1886 (1986).

[15] G.S. Uhrig and H.J. Schulz, Phys. Rev. B **54**, R9624 (1996).

[16] K.Damle and S.E.Nagler (unpublished).

[17] G. Bouzerar, A.P. Kampf, and G.I. Japaridze, cond-mat/9801046, 1998 (unpublished).

[18] A. Fledderjohann and C. Gros, Europhys. Lett. **37**, 189 (1997).

[19] D. Poilblanc, J. Riera, C. A. Hayward, C. Berthier, and M. Horvatić, Phys. Rev. B **55**, 11 941 (1997).

[20] K.M. Diedrix, H.W.J. Blöte, J.P. Groen, T.O. Klassen, and N.J. Poulis, Phys. Rev. B **19**, 420 (1979).

[21] T. Barnes and J. Riera, Phys. Rev. B **50**, 6817 (1994).

[22] A. Brooks Harris, Phys. Rev. B **7**, 3166 (1973).

[23] B.N.Parlett, *The Symmetric Eigenvalue Problem* (Prentice-Hall, Englewood Cliffs, NJ, 1980).

[24] D. Bailey, ACM Trans. Math. Softw. **19**, 288 (1993).

[25] E. Dagotto and A. Moreo, Phys. Rev. D **31**, 865 (1985); E. Gagliano, E. Dagotto, A. Moreo, and F. Alcaraz, Phys. Rev. B **34**, 1677 (1986); **35**, 8562(E) (1987).

[26] S. White, Phys. Rev. Lett. **69**, 2863 (1993); Phys. Rev. B **48**, 10 345 (1993).

[27] D.A. Tennant, S.E. Nagler, A.W. Garrett, T. Barnes, and C.C. Torardi, Phys. Rev. Lett. **78**, 4998 (1997).

[28] R.S. Eccleston, M. Uehara, J. Akimitsu, H. Eisaki, N. Motoyama, and S. Uchida, cond-mat/9711053 (unpublished); see also M. Matsuda and K. Katsumata, Phys. Rev. B **53**, 12 201 (1996); M. Matsuda, K .Katsumata;, H. Eisaki, N. Motoyama, S. Uchida, S.M. Shapiro, and G. Shirane, *ibid.* **54**, 12 199 (1996); M. Matsuda, K. Katsumata, T. Yokoo, S.M. Shapiro, and G. Shirane, *ibid.* **54**, R15 626 (1996); M. Matsuda, K. Katsumata, T. Osafune, N. Motoyama, H. Eisaki, S. Uchida, T. Yokoo, S.M. Shapiro, G. Shirane, and J.L. Zarestky, *ibid.* **56**, 1 (1997).

[29] K.M. Diedrix, J.P. Groen, L.S.J.M. Henkens, T.O. Klassen, and N.J. Poulis, Physica B **93**, 99 (1978); D.B. Brown, J.A. Donner, J.W. Hall, S.R. Wilson, D.J. Hodgson, and W.E. Hatfield, Inorg. Chem. **18**, 2635 (1979); J.C. Bonner, S.A. Friedberg, H. Kobayashi, D.L. Meier, and H.W.J. Blöte, Phys. Rev. B **27**, 248 (1983).

[30] G. Castilla, S. Chakravarty, and V.J. Emery, Phys. Rev. Lett. **75**, 1823 (1995). $CuGeO_3$ appears to have a large second nearest neighbor magnetic coupling; see also J. Riera and A. Dobry, Phys. Rev. B **51**, 16 098 (1995).

[31] B. Lake, Ph.D. thesis, Oxford University, 1997; B. Lake, R.A. Cowley, and D.A. Tennant, J. Phys.: Condens. Matter **9**, 10 951 (1997); J.P. Doumerc, J.M. Dance, J.P. Chaminade, M. Pouchard, P. Hagemuller, and M. Krussanova, Mater. Res. Bull. **16**, 985 (1981).

[32] M. Isobe and Y. Ueda, J. Phys. Soc. Jpn. **65**, 1178 (1996); D. Augier, D. Poilblanc, S. Haas, A. Delia, and E. Dagotto, Phys. Rev. B **56**, R5732 (1997) .

[33] E.M. McCarron III, M.A. Subramanian, J.C. Calabrese, and R.L. Harlow, Mater. Res. Bull. **23**, 1355 (1988); T. Siegrist, L.F. Schneemeyer, S.A. Sunshine, J.V. Waszczak, and R.S. Roth, *ibid.* **23**, 1429 (1988).

[34] A.W. Garrett, S.E. Nagler, D.A. Tennant, B.C. Sales, and T. Barnes, Phys. Rev. Lett. **79**, 745 (1997).